

Temperature Field Simulation of Submarine Cable under Different Laying Environments Based on COMSOL

Guozhu Wang^{1,2,*}, Yajun Zhang^{1,2}, and Zhichao Qiao³

¹School of Cable Engineering, Henan Institute of Technology, Xinxiang 453003, China

²Key Laboratory of Cable Structure and Materials in Henan Province, Xinxiang 453003, China

³Far East Cable Co. Ltd, Wuxi 214000, China

ABSTRACT: With the increasing maturity of marine energy development technology, the application ratio of submarine cable in marine engineering is climbing. The connection of submarine cable between offshore wind farms and mainland power grids is of great significance, and temperature is an important indicator for evaluating the safe operation status, which affects the stability and reliability of the cable directly. When the cable load exceeds the rated range, it will lead to a sharp rise in temperature, which will not only shorten its service life, but also may trigger an electrical fault. At lower loads, the cable fails to make full use of its transmission capacity under the rated load, thus affecting the economy of power supply. Therefore, the control of temperature rise of transmission lines during long-term operation is particularly critical, which is related to the stable operation of the power grid and the safety of power supply directly. This study conducted a detailed calculation of the current carrying capacity of submarine cable in accordance with the IEC60287 standard and simulated the temperature field distribution of HYJQF41-F-26/35 kV $3 \times 70 \text{ mm}^2$ three core AC submarine cable in different laying environments using COMSOL simulation software, providing a scientific basis for the structural design and material selection of three core submarine cable.

1. INTRODUCTION

As the core carrier of cross ocean energy transmission, the safe operation of submarine cable is directly related to the reliability of ocean energy development. Research has shown that when the working current of submarine cable exceeds the rated current carrying capacity, the temperature of the conductor will sharply rise, leading to accelerated aging of the insulation layer [1–3], and it can also cause thermal breakdown faults in severe cases. However, the allowable current carrying capacity of submarine cable is not a fixed value but is dynamically influenced by multiple factors such as laying method, environmental temperature, and soil thermal resistance [4–7]. “Directly buried” refers to the method of laying cables directly into the soil. This laying method usually involves excavating trenches, placing cable into the soil, and then backfilling. With “directly buried”, the soil thermal resistance coefficient (usually $0.5\text{--}1.2 \text{ K} \cdot \text{m/W}$) is significantly higher than that of the air medium, resulting in a decrease of about 30% in download flow under the same working conditions [4, 8–10]. Therefore, accurately evaluating the distribution pattern of current carrying capacity under different laying scenarios is crucial for optimizing the design and operation strategies of submarine cable engineering.

This study breaks through the traditional static analysis framework and constructs a multi-physics coupled simulation model, revealing the dynamic impact mechanism of laying methods on the temperature field of submarine cable system-

atically. This study uses COMSOL simulation software to analyze the temperature field distribution during the operation of submarine cable in three laying methods: direct burial, protective pipe laying, and cable trench laying, and takes HYJQF41-F-26/35 kV $3 \times 70 \text{ mm}^2$ submarine cable as an example for finite element analysis. The structure of submarine cables is illustrated in Fig. 1. COMSOL simulation software was used to construct a temperature field calculation model for three core AC submarine cable under different laying

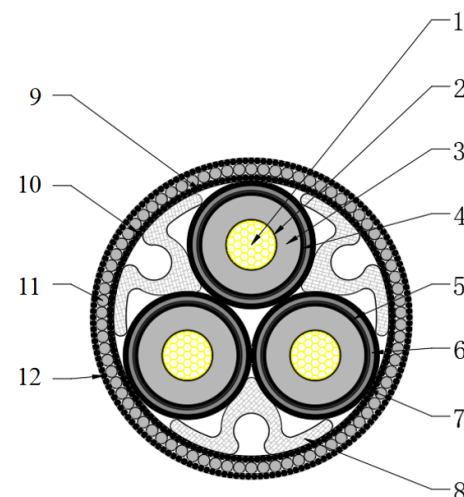


FIGURE 1. HYJQF41-F-26/35 kV $3 \times 70 \text{ mm}^2$ submarine cable structure diagram.

* Corresponding author: Guozhu Wang (wang.guo.zhu@163.com).

methods. In the direct burial method, coupling analysis of electromagnetic and thermal fields was conducted. Thermal field was conducted under the conditions of protective pipe laying and cable trench laying, and the effect of air flow on the temperature field distribution of submarine cable was explored.

This study systematically reveals the nonlinear impact of laying methods on the current carrying capacity of submarine cable through high-precision multi-physics coupling modeling. The proposed refined simulation method and engineering optimization strategy provide important technical support for the construction of deep-sea energy corridors. Future work will expand to the study of multi-system coupling in the linkage of submarine cable and underwater observation networks.

2. SUBMARINE CABLE MODELING

2.1. Mathematical Model of Electromagnetic Field

When current passes through the cable (except for the influence of displacement current), a stable electromagnetic environment is generated around the cable [8–11] and its electromagnetic field as Eqs. (1)–(3).

$$B = \mu H \quad (1)$$

$$D = \varepsilon E \quad (2)$$

$$J = \sigma E \quad (3)$$

where B represents the vector of magnetic induction intensity, H the magnetic field strength vector, D the vector of electric flux density, E the electric field strength vector, J the vector of conduction current density, ε the dielectric constant, μ the magnetic permeability, and σ the conductivity.

According to the fundamental principles of electromagnetism, electromagnetic phenomena near cable areas can be explained using Maxwell's Eq. (4).

$$\begin{cases} \nabla \cdot D = \rho \\ \nabla \cdot B = 0 \\ \nabla \times E = -\frac{\partial B}{\partial t} \\ \nabla \times H = J + \frac{\partial D}{\partial t} \end{cases} \quad (4)$$

This article studies the distribution characteristics of the temperature field inside the cable. Therefore, in the constructed equation, the first equation embodies Gaussian law; the second equation indicates the continuity of the magnetic field; the third equation is based on Faraday's law of magnetic field; the fourth equation is calculated according to Ampere's law of circuits [11–15]. On the basis of Maxwell's equations, derive Eq. (5) for magnetic potential vectors in different media layers.

On the plane XOY , substituting Eq. (5) into Eq. (4) yields the vector magnetic potential Eq. (6).

$$B = \nabla \times A = \frac{\partial A_z}{\partial y} i - \frac{\partial A_z}{\partial x} j \quad (5)$$

$$\nabla^2 A_z = \frac{\partial^2 A_z}{\partial x^2} + \frac{\partial^2 A_z}{\partial y^2} = -\mu_0 J_z \quad (6)$$

where A_z represents the vector magnetic potential corresponding to each layer; J_z indicate the current density at each layer of cable material. The material vector magnetic potential equation for each layer can be derived from Eq. (6). However, for the insulation layer, outer protective layer, and other parts of the cable, because the current density inside is 0, the vector magnetic potential equation can be simplified as Eq. (7).

$$\nabla^2 A_z = 0 \quad (7)$$

2.2. Mathematical Model of Heat Transfer Field

This article describes the temperature distribution relationship between cable and its surrounding media by constructing a differential equation for the thermal conductivity of cable. For this problem, it is also necessary to establish appropriate boundary conditions and time factors to form a complete mathematical model [14–17].

Simplify the cable into a thermal conductor with a heat source. Select a micro unit cell for energy balance analysis as shown in Fig. 2. According to the principle of energy conservation, the heat balance relationship Eq. (8) for micro unit cell is obtained.

$$d\phi_{in} + dQ = d\phi_{out} + dU \quad (8)$$

where ϕ represents the heat generated and dissipated per unit volume per unit time.

To accurately obtain the temperature field inside the cable, it is necessary to establish corresponding heat transfer equations. In addition, special boundary conditions that can describe the heat transfer and heat transfer characteristics at the cable interface need to be provided. When solving the temperature field of a three core AC submarine cable, it can be summarized into three different boundary conditions. Three boundary con-

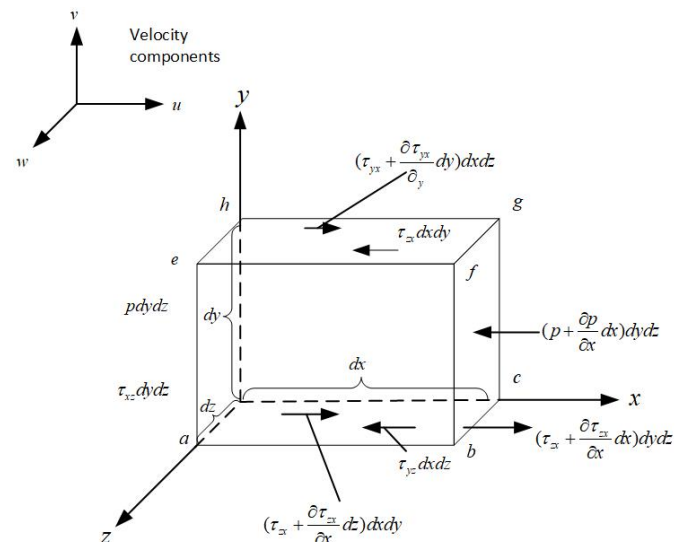


FIGURE 2. Thermal balance analysis diagram of conductor.

ditions are represented by Eqs. (9)–(11):

$$T|_{t=0} = \varphi(x, y) \quad (9)$$

$$T|_{\tau} = f(x, y, t) \quad (10)$$

$$-k \frac{\partial T}{\partial n}|_{\tau} = g(x, y, t) \quad (11)$$

where $\varphi(x, y)$ represents the temperature distribution corresponding to the solution region of the known temperature field; τ represents the boundary of the micro unit cell; $f(x, y, t)$ is the temperature distribution corresponding to the boundary solution area with known temperature; $g(x, y, t)$ is the vector function of heat flux density at the boundary [18, 19].

2.3. Mathematical Model of Fluid Field

For the laying method of cable trenches and protective pipes, considering the convective and thermal conductivity characteristics of the air medium, a fluid dynamics model needs to be constructed. This model needs to follow the laws of conservation of mass, momentum, and energy to accurately describe the heat transfer process within the air layer, as shown in Eq. (12):

$$\frac{\partial u}{\partial x} + \frac{\partial v}{\partial y} + \frac{\partial w}{\partial z} = 0 \quad (12)$$

Based on previous assumptions, it is assumed that the viscosity coefficient of the fluid can be neglected when the temperature field of cable trenches and protective pipes are studied. According to the principle of conservation of fluid momentum, the momentum equation of the air layer is derived, and Eq. (13) is given.

$$\begin{cases} \rho \left(u \frac{\partial u}{\partial x} + v \frac{\partial u}{\partial y} + w \frac{\partial u}{\partial z} \right) = -\frac{\partial \rho}{\partial x} + \eta \left(\frac{\partial^2 u}{\partial x^2} + \frac{\partial^2 u}{\partial y^2} + \frac{\partial^2 u}{\partial z^2} \right) \\ \quad + pga (T - T_{\tau}) \cos \theta \\ \rho \left(u \frac{\partial v}{\partial x} + v \frac{\partial v}{\partial y} + w \frac{\partial v}{\partial z} \right) = -\frac{\partial \rho}{\partial y} + \eta \left(\frac{\partial^2 v}{\partial x^2} + \frac{\partial^2 v}{\partial y^2} + \frac{\partial^2 v}{\partial z^2} \right) \\ \quad + pga (T - T_{\tau}) \cos \theta \\ \rho \left(u \frac{\partial w}{\partial x} + v \frac{\partial w}{\partial y} + w \frac{\partial w}{\partial z} \right) = -\frac{\partial \rho}{\partial z} + \eta \left(\frac{\partial^2 w}{\partial x^2} + \frac{\partial^2 w}{\partial y^2} + \frac{\partial^2 w}{\partial z^2} \right) \\ \quad + pga (T - T_{\tau}) \end{cases} \quad (13)$$

Based on certain premises, when considering the laying of cable trenches and protective pipes, it is assumed that the air viscosity coefficient can be ignored. According to the principle of fluid energy conservation, derive the energy differential equation of the gas layer, as shown in Eq. (14):

$$u \frac{\partial T}{\partial x} + v \frac{\partial T}{\partial y} + w \frac{\partial T}{\partial z} - \lambda \left(\frac{\partial^2 T}{\partial x^2} + \frac{\partial^2 T}{\partial y^2} + \frac{\partial^2 T}{\partial z^2} \right) = 0 \quad (14)$$

3. CALCULATION OF CURRENT CARRYING CAPACITY OF SUBMARINE CABLE

Using finite element analysis to analyze the temperature field of submarine cables requires establishing different models for different laying environments. To simplify the calculation, this article selects a certain cross-section of the submarine cable for temperature field research. When the cable is buried directly, a natural convection heat transfer occurs between its outer surface and the surrounding soil. When the cable is laid in the cable trench, the heat transfer between the cable trench cover and external atmospheric medium is also natural convection heat transfer.

The calculation of the temperature field of submarine cable first requires determining the boundary conditions of no temperature change at the bottom, no temperature in side, and the presence of gas at the top. The calculation of submarine cable laying areas using finite element method is relatively cumbersome. Therefore, the area to be solved will be partitioned, and then each modular grid will be analyzed. After partitioning the studied area, the analysis of each node was merged into a complete linear equation for solution, and the temperature distribution of each node was obtained. The basic process of using finite element method to solve the temperature field of cable is shown in Fig. 3.

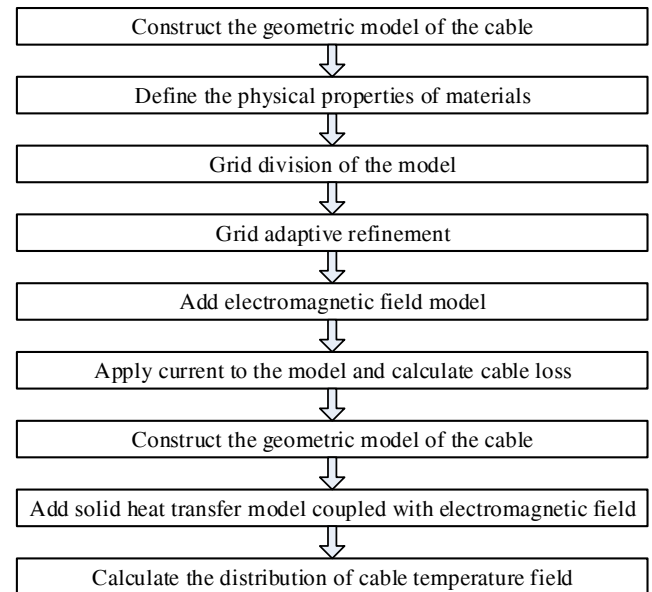


FIGURE 3. Modeling process diagram.

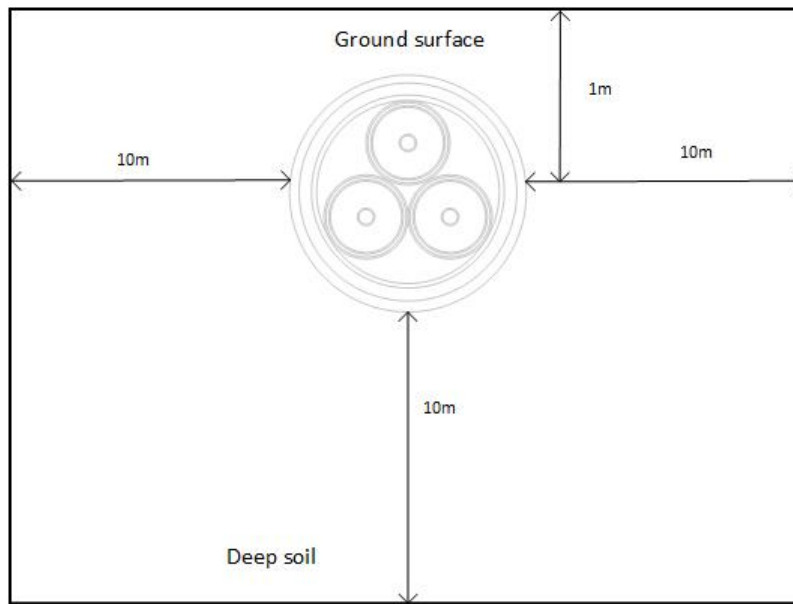
4. CALCULATION OF TEMPERATURE FIELD OF SUBMARINE CABLE UNDER DIFFERENT LAYING ENVIRONMENTS

4.1. Calculation of Temperature Field for Underwater Direct Burial Laying

The submarine cable model studied in this article is HYJQF41-F-26/35 kV $3 \times 70 \text{ mm}^2$. The parameters of the submarine cable are shown in Table 1. The current carrying capacity of a single circuit buried installation was calculated using finite element

TABLE 1. Cable structure parameters and material parameters.

Structure name	Radius (mm)	Thermal conductivity (W/m*K)	Conductivity (S/m)	Relative dielectric constant
Copper conductor	5.00	400	5.998×10^7	1
XLPE	16.30	0.2857	1×10^{-15}	2.5
Semi conductive buffer waterproof tape	17.75	0.1429	1×10^{-16}	2.4
Lead alloy sleeve	17.95	34.8	4.81×10^6	1
Semi conductive PE sheath	21.75	0.2857	1×10^{-15}	2.25
PP filling strip	49.75	0.2857	1×10^{-15}	2.25
Steel wire armor layer	54.75	44.5	4.032×10^6	1
Outer sheath layer	58.75	0.1667	1×10^{-16}	8

**FIGURE 4.** Geometric model diagram of single circuit AC three core submarine cable directly buried laying.

method and compared with the results of equivalent thermal resistance method to verify the accuracy of the finite element model. Using COMSOL simulation software, a submarine cable coupling model is constructed as shown in Fig. 4.

In the process of laying buried cable, the solution area of the cable is set to three boundary conditions [20]. The boundary conditions of the submarine cable are divided, and the soil surface boundary is classified as the third type of boundary condition due to its exchange with the external environment and convective heat. In theory, the boundary of the soil should be set at infinity. However, through calculations, it was found that the heat generated by the cable has minimal impact on the soil beyond a distance of 10 meters, and its change in soil temperature gradient can be ignored. Therefore, the actual soil temperature gradient is considered zero, thus defining the second type of boundary condition. The bottom soil layer is less affected by cable heat and has little temperature change, so its temperature can be regarded as a constant. In this study, the temperature

of the bottom soil was set to 20° as the first type of boundary condition.

After building the model, iterative methods can be used to analyze the current carrying capacity and temperature distribution of the cable. The detailed steps are as follows:

- (1) By writing Matlab models that comply with IEC60287 and IEC60285 standards, calculate the current carrying capacity of the submarine cable and input the current carrying capacity values into COMSOL. Set the maximum temperature of the conductor in COMSOL to 90° and conduct parameterized scanning.
- (2) Determine the initial current value I_0 for iterative calculation based on the parameterized scan results. Establish a discriminant function “maxop” and relative tolerance value within the software. The initial value I_0 of this model of submarine cable is set to 270A, and the relative tolerance is set to 0.01.

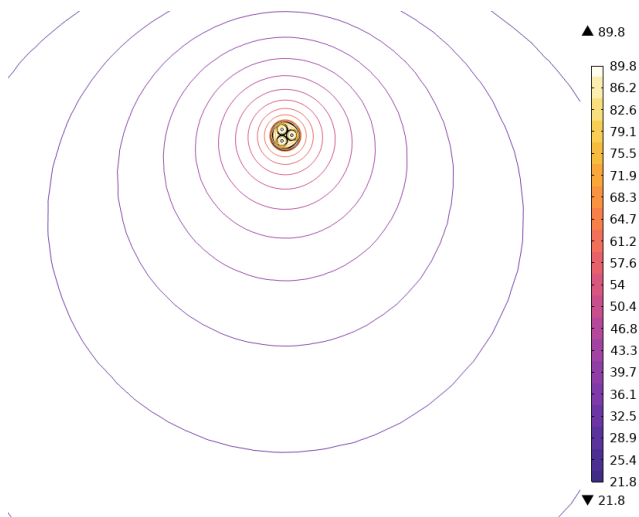


FIGURE 5. Temperature field distribution of single loop AC three core submarine cable.

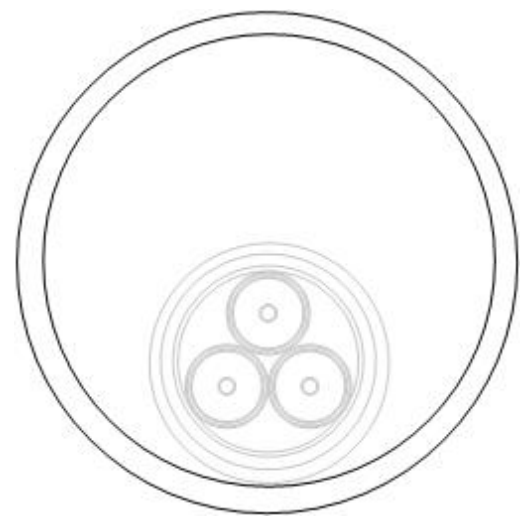


FIGURE 6. Pipe laying model of submarine cable.

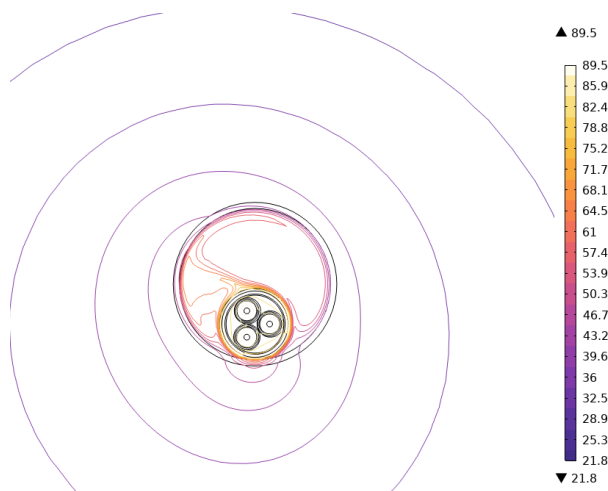


FIGURE 7. Temperature distribution of submarine cable under pipe laying conditions.

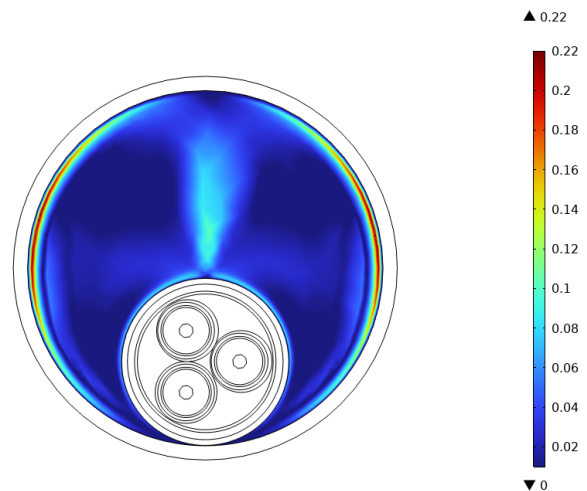


FIGURE 8. Installation pipe air flow distribution diagram of submarine cable.

- (3) Set up a probe inside the core conductor and start iterative calculation. Compare the temperature of the core conductor recorded by the probe with “Maxtemp”, and end the operation when the absolute value of the difference is not greater than the relative tolerance.

Figure 5 shows the temperature distribution of the surrounding medium of the core conductor at 90° . The main heat source for submarine cable heating is the working conductor core, so its temperature is the highest, and the temperature gradually decreases from the core to the outer surface of the cable. Similarly, the temperature of the external medium soil also gradually decreases with the increase of distance from the conductor core.

The laying method of submarine cables on land is pipe laying. At this point, the cable needs to pass through a plastic pipe set underground. Given the presence of air inside the pipe, we can calculate that the flow of air inside the pipe will affect the

heat dissipation effect of the cable. This study still selects cable as the core research object and constructs a geometric model based on the single circuit laying mode, as shown in Fig. 6.

Due to the presence of air in the pipe, heating will cause flow phenomena. Fig. 7 shows the stable flow of air in the pipe at a certain current carrying capacity, from which the maximum air velocity can be obtained as 0.22 m/s. The temperature of the cable conductor increases, and the air flow inside the pipe becomes more intense, which helps to dissipate heat from the cable by taking away heat.

Figure 8 shows the distribution of air flow inside the installation pipe of submarine cable. Compared to the direct burial method in soil, the maximum temperature of the cable core has decreased. Focusing on the modeling and simulation research of submarine cable, Fig. 9 shows the geometric model under single loop laying in this model, and the cable is placed on the supports of the ditch, with a distance of 250 mm between the

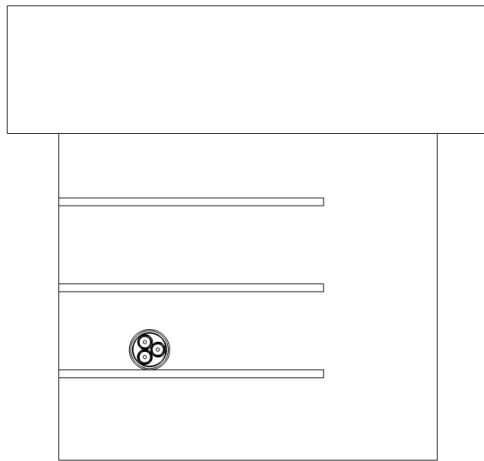


FIGURE 9. Model diagram of laying three core submarine cable trench for communication.

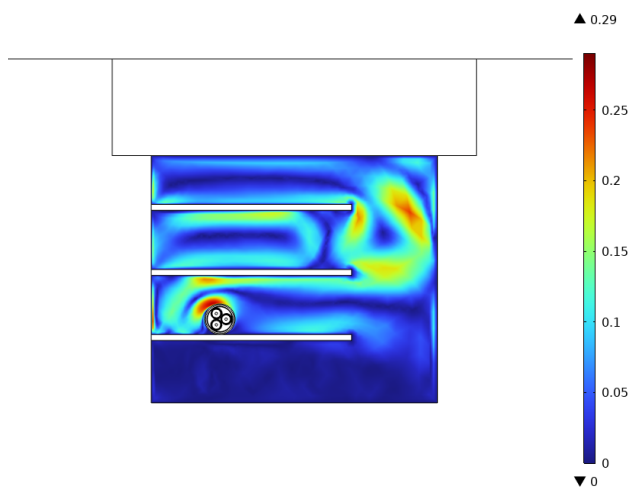


FIGURE 10. Temperature distribution of submarine cable during cable trench laying.

supports. The inside of the ditch is filled with air, while the outside is surrounded by soil. Maintain a distance of 10 m between the left, right, and bottom boundaries of the solution area and the outer wall of the cable trench. Above the ditch is the cover plate of the cable trench, which is in direct contact with the external air medium. The structure and environmental parameters of the cable are the same as those listed in Table 1.

For the same laying environment, we compared the current carrying capacity calculated by the equivalent thermal resistance method with the current carrying capacity data provided by the Far East submarine cable.

There are two main factors that cause errors when two sets of data are compared:

- (1) Traditional calculation methods have not taken into account the significant impact of air flow in cable trenches on cable heat dissipation. During simulation calculations, air flow velocity is usually omitted, which makes the empirical formula based equivalent thermal resistance method

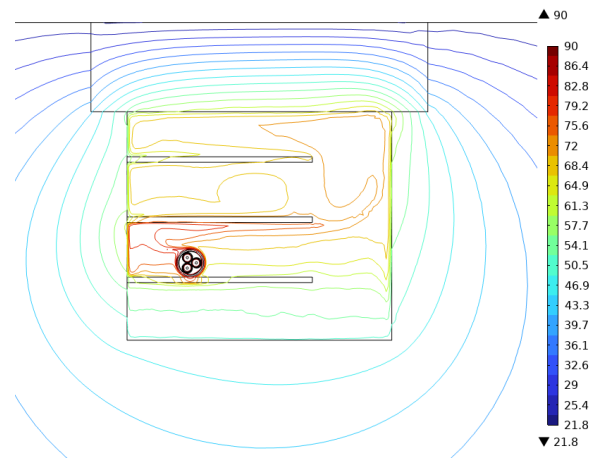


FIGURE 11. Distribution of air flow during the laying of submarine cable in cable trenches.

unable to accurately reflect the aerodynamic characteristics inside the cable trench.

- (2) Due to the relatively spacious space of the cable trench, the heat generated by the cables causes drastic changes in the air flow inside the trench, thereby taking away most of the heat. Meanwhile, the cover plate of the cable trench has good heat dissipation performance, which can effectively transfer heat to the external air.

Figure 10 shows the temperature distribution of submarine cable in the cable trench. Due to the presence of air in the cable trench, heating can cause air flow. Fig. 11 shows the distribution of air flow in the cable trench. By observing the image, it can be determined that the maximum velocity of the air reaches 0.29 m/s.

5. CONCLUSION

This study focuses on submarine cable and verifies the computational accuracy of the coupled model through experiments. Furthermore, we also constructed a computational model for the single circuit pipe laying and cable trench laying of submarine cable involving electromagnetic fields, heat transfer fields, and fluid fields. Each structural material of submarine cable has its own temperature resistance limit. Therefore, in the process of power transmission and distribution, it is crucial to choose an appropriate current to ensure that the heat generated does not cause damage to the cable structure and materials. Accurately calculating the current carrying capacity of submarine cable is essential. This study uses the IEC60287 equivalent thermal resistance method to analyze and compare the current carrying capacity and temperature field of submarine cable, and calculates the current carrying capacity of cable under different laying modes and burial depths. A set of electromagnetic field heat transfer field volume calculation models for submarine cable was established using COMSOL numerical simulation method and finite element method.

Based on the simulation results, the applicable scenarios of the three laying methods can be summarized as follows:

- (1) Direct burial method is economically efficient and recommended for long-distance submarine trunk lines.
- (2) The protective management method is applicable to situations with medium distance and the need to prevent external damage.
- (3) The cable trench method is particularly suitable for engineering scenarios with short distances, high load requirements, or periodic maintenance due to its excellent heat dissipation performance.

ACKNOWLEDGEMENT

This research was supported by the Joint Fund of Henan Science and Technology Research and Development Plan in 2023 (No. 232103810028).

REFERENCES

- [1] He, F., Y. L. Zhang, S. R. Wei, *et al.*, "Planning of large-scale offshore wind farm cluster access system considering grid-connected flexibility," *Smart Power*, Vol. 52, No. 9, 33–40, 2024.
- [2] Wu, B. J., R. R. Ding, C. Chen, *et al.*, "Simulation on current capacity and temperature field distribution in 220 kV XLPE submarine cable under low frequency," *Insulation Material*, Vol. 56, No. 12, 34–42, 2023.
- [3] Li, X. F. and X. J. Tang, "Analysis of high voltage XLPE submarine cable current carrying capacity," *Guangdong Power Transmission and Transformation Technology*, Vol. 12, No. 6, 39–42, 2010.
- [4] Su, J. M., Y. W. Tang, and Y. L. Chen, "Research and comparison of calculation methods for current carrying capacity of composite submarine cables," *Modern Computers*, Vol. 24, No. 8, 26–31, 2018.
- [5] Zhao, L., X. Zhao, T. Li, *et al.*, "Design and selection of ± 160 kV XLPE insulated cable system for multi-terminal VSC HVDC power transmission system," *High Voltage Engineering*, Vol. 40, No. 9, 2635–2643, 2014.
- [6] Liu, C. and X. Zheng, "Design on calculation software for temperature field and ampacity of electric power cable," *Guangdong Electric Power*, Vol. 28, No. 6, 53–61, 2015.
- [7] Qiao, J., X. Zhao, Y. Xia, *et al.*, "Simulation analysis of steady-state ampacity of ± 500 kV high-voltage DC submarine cables under different laying methods," *High Voltage Engineering*, Vol. 49, No. 2, 597–607, 2023.
- [8] Zheng, M., Q. N. Hu, and G. Liu, "Comparative analysis of download flow for different laying methods of 110 kV submarine cables," *Electrical Applications*, Vol. 33, No. 23, 146–149, 2014.
- [9] Liu, P. P., B. W. An, L. Zhou, *et al.*, "Simulation of temperature field of composite submarine cable based on finite element method," *Computer Simulation*, Vol. 30, No. 10, 288–292, 2013.
- [10] Zhang, S. G., X. M. Guo, C. S. Zhang, *et al.*, "Analysis on temperature field of high voltage DC submarine cable in different laying environment," *Guangdong Electric Power*, Vol. 29, No. 1, 102–107, 2016.
- [11] Le, Y., L. Sun, W. Peng, *et al.*, "Analysis and simulation research on current carrying capacity bottleneck of typical AC high-voltage submarine cable project," *High Voltage Apparatus*, Vol. 58, No. 1, 70–78, 2022.
- [12] Zhang, Y., X. Chen, H. Zhang, J. Liu, C. Zhang, and J. Jiao, "Analysis on the temperature field and the ampacity of XLPE submarine HV cable based on electro-thermal-flow multiphysics coupling simulation," *Polymers*, Vol. 12, No. 4, 952, 2020.
- [13] Liu, N. and J. M. Liu, "Simulation analysis of thermal effects of DC submarine cables based on COMSOL," *Jilin Water Resources*, Vol. 9, 6–8, 2019.
- [14] Duan, J. B., C. Q. Yin, A. Q. Lv, *et al.*, "Analysis method for temperature of high voltage submarine cable based on IEC 60287 and finite element," *High Voltage Apparatus*, Vol. 50, No. 1, 1–6, 2014.
- [15] Zhang, L., Y. Xuan, Y. Le, *et al.*, "Ampacity calculation, temperature simulation and thermal cycling experiment for 110 kV submarine cable," *High Voltage Apparatus*, Vol. 52, No. 6, 135–140, 2016.
- [16] Liu, J., X. J. Li, H. Gao, *et al.*, "Electric field and temperature field characteristics of subsea umbilical cable based on finite element method," *High Voltage Engineering*, Vol. 40, No. 6, 1658–1665, 2014.
- [17] Ying, Q., "The prospect of development of DC submarine cables in China," *Electric Wire & Cable*, Vol. 3, 1–7, 2012.
- [18] Chen, Q., Y. Qin, N. Shang, M. Chi, and X. Wei, "Influence analysis of temperature on electric-field distribution in HVDC cable joint," *High Voltage Engineering*, Vol. 40, No. 9, 2619–2626, 2014.
- [19] Liu, P., S. Yu, Y. L. Chen, *et al.*, "Study of boundary conditions in temperature field model of composite submarine cable," *Measurement and Control Technology*, Vol. 34, No. 5, 114–117, 2015.
- [20] Lv, A., X. Kou, C. Yin, *et al.*, "Modeling of temperature relation between optical fiber and conductor in 3-core submarine power cable," *Transactions of China Electrotechnical Society*, Vol. 31, No. 18, 59–65, 2016.